2024 IEEE/RSJ International Conference on Intelligent Robots and Systems (IROS)
October 14-18, 2024. Abu Dhabi, UAE

Modernising Delivery: A Low-Energy Tethered Package System Using Fixed-Wing Drones

Samuel Ord[1], Matthew Marino[2] and Timothy Wiley[3]

***Abstract*— Fixed-wing Uncrewed Aerial Vehicles (UAVs) can be used for remote package delivery missions by connecting a package to a UAV via a long tether. With a circular flight path at a calculated loiter radius, tether length and orbiting velocity, a package can be lowered to the ground in a quasi-stationary manner. This method achieves this with significantly less energy than hybrid hovering aircraft, which are currently used. UAV operating limitations pose a challenge for this method as ensuring the package stabilises such that it can be safely deployed without damage or posing a risk to people or property is challenging in most environmental conditions. To improve tether and package stabilisation, we introduce a novel Mid-Tether Drag Device (MTDD) which enables compliant delivery missions within regulatory frameworks. We present a mathematical model of the delivery with a UAV and MTDD. We verify the accuracy of our model with real-world flight tests in low wind conditions without the MTDD, which have not been previously conducted at this scale in literature. Further validation is presented with flight tests at a flight range using a UAV instrumented with a package deployment system with both UAV and package tracking data acquisition. Our work enhances the abilities of UAVs to conduct aerial package delivery.**

I. Introduction

Uncrewed Aerial Vehicles (UAVs) are a steadily growing part of the aerospace industry with various use cases. In the logistics sector, UAVs improve delivery times and offer a new and environmentally friendly method of package delivery [1]. With the rapid rise of online purchases [2], UAVs can avoid road congestion for uninterrupted delivery missions and have a greater growth potential compared with ground-based deliveries. Commercial development [3] currently focuses on multi-rotor systems in urban environments, with Vertical Take-Off and Landing (VTOL) capabilities. While multi-rotor UAVs are suitable for urban small package delivery missions, they are limited by their battery, affecting range and payload capacity, which are significant for long-range missions. Hybrid VTOL vehicles have shown promise in expanding the capability of UAV package delivery as they can offer longer range and payload capacity. This has been proven in large scale operational trials in Australia [4] where small household items can be delivered via a phone app with a VTOL UAV. However, these aircraft still require a hover state to deliver packages, which consumes a substantial proportion of the battery capacity. Fixed-wing UAVs can offer package and range capabilities that go beyond those of hovering aircraft. Due to the low-energy cruise state of a fixed-wing aircraft, endurance is significantly extended, and thus, multiple packages can be delivered in a single flight mission. Fixed-wing UAVs operate with the least energy usage compared to other aircraft configurations as they have no hover or high-power flight phases [5]. However, without a landing strip at the delivery site, the package must be "delivered" from the UAV while in flight by either dropping the package via parachute or lowering the package to the ground via a tether. While both have trade-offs, we prefer the tethered approach as dropping a package from a UAV is risky within residential, urban or suburban settings. Current fixed-wing tether designs are unsuitable for UAV operation, especially in variable wind conditions. We present and experimentally evaluate a novel design of a tethered package delivery system (Figure 1) for a fixed-wing UAV by introducing a Mid-Tethered Drag Device (MTDD), which enables reliable package delivery in variable wind conditions.

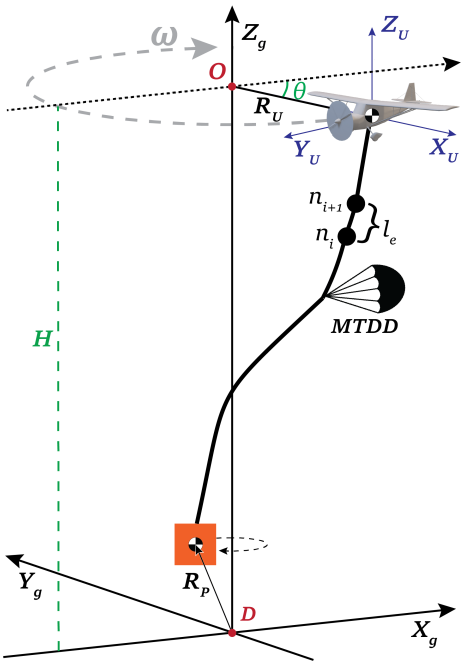

Fig. 1. Illustration of our tether package delivery design stabilising a package to a small orbital radius with a fixed-wing UAV, featuring a Mid-Tethered Drag Device

Saint [6], a pilot for the Missionary Aviation Fellowship in the 1950s, delivered supplies to Christian missionaries working among the Indian tribes in Ecuador, often in remote locations where landing was not possible. He devised a

[1] School of Engineering, RMIT University, samuel.ord@rmit.edu.au
[2] School of Engineering, RMIT University, matthew.marino@rmit.edu.au
[3] School of Computing Technologies, RMIT University, timothy.wiley@rmit.edu.au

delivery method by attaching a large canvas bag to a rope and slowly fed it from his plane as he flew in a circular orbit above the delivery location. Illustrated in Figure 1, the package with a sufficiently long tether stabilises to a small orbital loop, where it "hovers" near ground level and is safe for a human to physically "catch-and-detach" the package.

This concept is what we build upon. However, UAVs must also comply with the aerospace regulations they operate, which can be more restrictive than those of crewed aircraft. In most circumstances, regulations limit uncrewed aircraft to an altitude ceiling of 120 metres (400 feet) [7]. Existing research considers scenarios that are not legally permitted and indicates that the tether length should be maximised to achieve a sufficiently small and stable orbit for the package. As shown in Figure 5, we have found that to achieve appropriate delivery radii and comply with the $120m$ operating ceiling, the system must complete orbital turns that exceed normal safe operational limits of commercial UAVs.

We fill this gap by developing a MTDD which enables reliable package delivery within the above constraints. To aid real-world experimentation, we also develop a simulation of the tethered system to test the different variables. This simulation is validated experimentally on a small UAV with the package deployment system attached. The simulation can then be calibrated to real-world conditions where our MTDD design and its effects on the tether dynamics and package behaviour can be investigated. We aim to reduce the package orbital radius to an acceptable value of less than one metre while the UAV operates within flight limits and ICAO regulations. Our novel contributions are:

- The investigation of a MTDD for a tethered fixed-wing package delivery UAV that allows for stable delivery of a package in varying wind conditions within operational and legal restrictions.
- Simulation of the fixed-wing UAV delivery system both with and without the MTDD in various wind conditions.
- Field tests experimental results without the MTDD to validate the simulator.

II. Related Work

Saint [6] pioneered the concept of a tethered package delivery system for a fixed-wing aircraft. Subsequent studies investigate how to optimise the system across varying conditions and operating restrictions for *crewed* aircraft. Huang [8] proposes a steady-state numeric model that predicts the behaviour of the tether as an aircraft is flying a circular path. Their model shows that regions of multi-valued solutions exist in the steady state model, which can and should be avoided during operation. Huang suggests that the transition from straight flight to orbital flight should be gradual, with at least three orbits flown before the package orbit stabilizes. Additionally, they discussed the use of a stepped diameter towline, which can eliminate the multi-valued region and tow load. This towline has similar characteristics to the MTDD, where a larger diameter tether, and therefore drag, is attached to the UAV and a smaller one towards the package ends.

Skop & Choo [9] propose an equilibrium equation using non-dimensional analysis for a non-extendable and flexible tether with a fixed spherical mass as the package. They confirm Huang's findings that multi-valued solutions exist with certain parameters. Their model shows that to avoid these multi-valued solutions and have a small delivery radius, a larger ratio between the tether length and loiter radius results in preferable package radii. However, increasing this ratio is not viable for tethered UAV delivery designs as the ICAO restrictions prevent using a suitably long tether, and aircraft operating limits restrict the minimum orbital radius. Additionally, the models are not verified in real-world flight tests.

Additional considerations must be made towards using UAVs for tethered delivery missions. Merz *et al.* [10] provides insight into the design characteristics required for optimal performance. A low-wing loading design with a longer tether yields the best results. However, the altitudes and tether lengths mentioned are against the ICAO regulation and, therefore, currently unfeasible for UAV delivery. Merz *et al.* also investigate path planning strategies [11]–[13] for UAVs and the ability of the UAV to maintain circular orbits in windy conditions. They concluded that with wind velocities above $5m/s$, additional means of compensation are required for steady package hover. Trivailo & Williams [14], [15] analyse three crewed aircraft types: a P-3C Orion aircraft, a light recreational aircraft, and a high-performance military aircraft. Light recreational aircraft can achieve small package radii better due to better stall limits.

Lapthorne & Trivailo [16] note that a knot in their tether experiments, a simple form of a MTDD, reduces the delivery radius. The knot creates additional drag, causing the tether below this point to be more vertical and closer to the orbital centre. This concept has been minimally explored with no in-depth field testing. Our work extends this concept, investigates the impacts of an MTDD that produces higher aerodynamic drag and provides insight into how environmental conditions influence package behaviour.

III. Model and Methodology

Our design for a fixed-wing package delivery UAV, including our novel Mid-Tether Drag Device (MTDD), is depicted in Figure 1. A tether (such as a cable or rope) is attached at one end to the underside of a fixed-wing UAV. The other end of the tether is attached to a package (or payload) as a box. A MTDD in the form of a hemispherical parachute with a drag coefficient of 1.42 [17] is attached to the tether between the aircraft and the package. As the MTDD impacts the delivery phase of the mission, we focus our study on this mission phase, where the UAV circles above the delivery location with the tether fully extended. We assume an existing flight controller sufficiently maintains a circular orbit for the UAV and numerically model this design as described in the following section.

A. Model of Package Delivery Dynamics

Our model uses the discrete Lumped Parameter Model (LPM) and is based on existing models of tether systems [15], [18]. The delivery location, D, of the inertial frame of reference, (X_g, Y_g, Z_g), in Cartesian coordinates, defines the desired delivery location, with D being at ground level. By convention, the X_g and Y_g axes are co-planer with the ground plane, and the Z_g is upwards, giving altitude above the ground. The UAV maintains a circular orbit of radius, R_U, around origin, O, which is at altitude H. The local frame of reference of the UAV, (X_U, Y_U, Z_U) is described in Cartesian coordinates with Y_U along the conventional longitudinal axis of a fixed-wing UAV in the direction of motion, Z_U parallel to Z_g, and X_U defining a right-hand-rule coordinate frame point towards, O. The angle θ is defined as the angle between X_g and X_U, giving the effective location of the UAV in its orbit. The orbital "loiter" rate of the UAV around O is denoted as ω as radians of θ per second.

The tether is modelled by discretising it into a set of ordered nodes $N = \{n_0, \ldots, n_N\}$. Under the LPM approach, each node, $n_i \in N$, is a point mass connected by mass-less springs to adjacent nodes, n_{i-1} and n_{i+1}. The spring models the tether's elasticity (both tension and strain). The first node, n_0, attaches to the package, and the last node, n_N, attaches to the UAV. All the external forces on the tether are applied to each node, eliminating inertial coupling between elements. The tether segments' tensile, gravitational, and aerodynamic forces are lumped on each node. The tension, $\boldsymbol{T_i}$, in each element is calculated according to Hooke's law:

$$\boldsymbol{T_i} = \frac{EA}{\boldsymbol{l_e}}(\boldsymbol{l} - \boldsymbol{l_e}) \tag{1}$$

Where E is the young's modulus of the tether and A its cross-sectional area. The unstrained distance between each node, that is, the length of the tether segment before the application of forces, l_e, is equal such that $l_e = {}^{L_T}/_{N}$ where L_T is the total tether length. l donates the new element length after the application of forces. It will be assumed that $\boldsymbol{l} > \boldsymbol{l_e}$, such that the tether maintains tension for small motions around the equilibrium position. The total tension, $\boldsymbol{T_i^{total}}$, applied to the i^{th} node with respect to the body-fixed coordinate frame is:

$$\boldsymbol{T_i^{total}} = \boldsymbol{T_i}\frac{\boldsymbol{l_i}}{|\boldsymbol{l_i}|} - \boldsymbol{T_{i+1}}\frac{\boldsymbol{l_{i+1}}}{|\boldsymbol{l_{i+1}}|} \tag{2}$$

The gravitational force of each element is:

$$\boldsymbol{F_{g_i}} = -mg\boldsymbol{z_i} \tag{3}$$

The tether has diameter, d_t, and density, ρ_t, which can be used to determine the segment mass, m.

Finally, the aerodynamic forces, lift and drag, are calculated off the cross-flow principle presented in Heorner [17]. Lift and drag are summed together to get a resultant aerodynamic force, F_{aero}:

$$\boldsymbol{F_{aero_i}} = \boldsymbol{F_{L_i}} + \boldsymbol{F_{D_i}} \qquad i = 0, 1, 2, \ldots, N \tag{4}$$

Fig. 2. Experimental test set up during a flight mission before deployment of package

The MTDD is modelled as a hemispherical parachute with a drag coefficient of 1.42 [17] and a radius of $0.5m$. The MTDD is attached to the tether at a node, n_{MTDD}, where $MTDD \neq 0$ or N. The MTDD mass and aerodynamic drag are added to the node, n_{MTDD}, altering Equations 3 & 4:

$$\boldsymbol{F_{g_{n_{MTDD}}}} = -(m_{n_{MTDD}} + m_{MTDD})\ g\ \boldsymbol{z_{MTDD}} \tag{5}$$

$$\boldsymbol{F_{aero_{n_{MTDD}}}} = \boldsymbol{F_{L_{n_{MTDD}}}} + \boldsymbol{F_{D_{n_{MTDD}}}} + \boldsymbol{F_{D_{MTDD}}} \tag{6}$$

Where $m_{n_{MTDD}}$, $F_{L_{n_{MTDD}}}$ and $F_{D_{n_{MTDD}}}$ are the original mass and drag characteristics of the tether nodal element where the MTDD is positioned. The package is modelled similarly by adding its mass and aerodynamic drag to the tether node n_0.

B. Wind Modelling

To model environmental wind conditions, the LLLJP wind shear formula [19] is chosen as it provides wind velocities at any height, z, by:

$$\boldsymbol{u(z)} = \boldsymbol{u_{z_0}} \cdot \left(\frac{z}{z_0}\right)^{\alpha} \tag{7}$$

where, $u(z)$ is the wind velocity at height z, u_{z_0} is the reference wind speed at the reference altitude z_0, and α is the wind shear exponent. We set $\alpha = 0.2$ and $z_0 = H$ as we presume delivery missions are conducted in an open field without trees, and the wind velocity can be measured by the UAV. The wind velocity for each tether node is thus derived by setting z to the node's height. The nodal wind velocity and direction are then combined with the nodal velocity for use in the aerodynamic equations.

C. Simulation

We implemented our model in simulation in MATLAB and Simulink® [20]. We limit the simulation to only model the behaviour of the tether. Thus, the movement of node, n_N, is set to the movement of the UAV, and the simulation predicts the movement of all other nodes based on the mathematical model. We note that our model of the tether and environment conditions, and by extension our simulation, are ideal forms without variance of real-world conditions. Thus, the simulation will not exactly predict the dynamics of the UAV and package in a real-world condition. Instead, our model provides projections of the *range* of dynamics of the UAV and package across conditions.

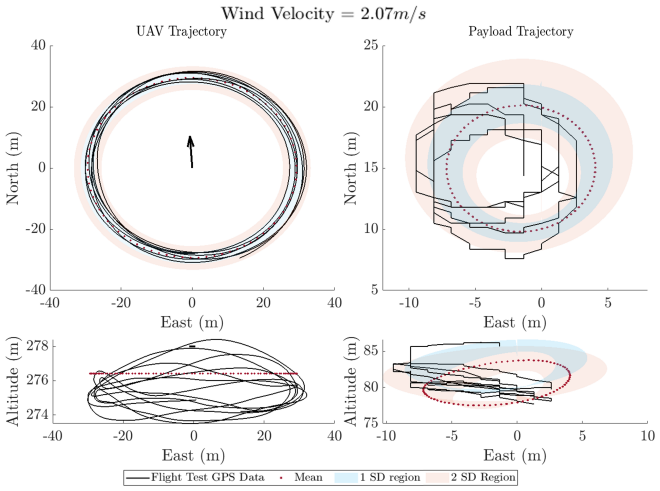

Fig. 3. UAV and package trajectory from experimental flight vs. averaged simulated conditions with a standard deviation of $1.94m$

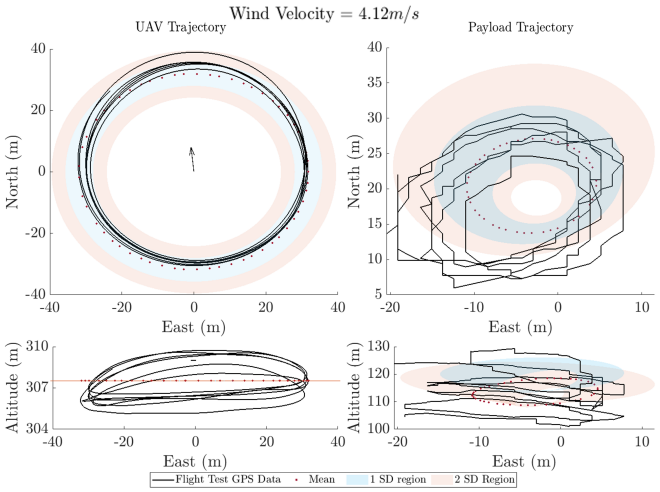

Fig. 4. UAV and package trajectory from experimental flight vs. averaged simulated conditions with a standard deviation of $3.84m$

IV. Real-World Field Test Results

First, we compare the simulator to real-world flight tests without the MTDD. These real-world field tests are conducted with a Phoenix Model Piper J3 Cub UAV, chosen for its sufficient manoeuvrability and carrying capacity. It is fitted with a Holybro Pixhawk® 6C flight controller flashed with ArduPilot (V4.4.4) [21]. This autopilot system has a loiter function that, when activated, will hold a circular flight path around a specified GPS location. During the experiments, the GPS position, airspeed, and flight surface controls of the UAV are tracked. Another flight controller is attached to the package, allowing us to gather GPS position data with accuracy similar to that of the UAVs.

The flight tests require the UAV to complete a full delivery mission, including take-off, delivery, and landing, even though the scope of this study is just the delivery phase. For this, we attach the package to the undercarriage of the UAV by a quick-release mechanism while retaining the tether within a spool, also attached to the UAV undercarriage, as shown in Figure 2. Approaching the loiter phase, a remote command drops the package through the quick-release mechanism, and the tether gradually unwinds. The UAV requires between two to three orbits after the loiter phase has begun to stabilise the cable and package. After the delivery mission, the tether is released from the UAV via a second quick-release mechanism, where the UAV can land safely. All experiments are conducted under strict safety rules at a controlled airfield.

To verify our model and simulation, we conducted 12 flight tests in light wind conditions, which can be defined as under three on the Beaufort scale [22]. We present two flights here, with the other flights following similar trends. The first test is conducted in a light breeze ($2.07\,m/s$), and the second in a gentle breeze ($4.12\,m/s$). Figures 3 and 4 show the UAV and package trajectories for the light and gentle wind conditions, respectively. The top two plots are from a top-down North-East perspective, and the bottom two plots show a side-on East-Down perspective to showcase altitude variation experienced by the package. The trajectory of the UAV is the left plot, and the package is the right plot. In each plot, the solid black line shows the recorded GPS trajectory of the UAV and package. The average loiter and velocity of the UAV and the average wind velocity and direction during the mission were used in the simulation. The trajectory of this flight path is illustrated with the dotted red line in the centre of the shaded regions, with the arrow indicating the direction of the wind, with the velocity noted in the title. The simulation model predicts where the package is orbiting based on this mean loiter radius and up to two standard deviations from the mean. These are represented by the blue and orange shaded regions in Figure 3 & 4.

In both flight tests, the UAV does not maintain a perfectly circular orbit, with slight variations in its flight path per rotation. This variation impacts the package, which also wanders in a non-circular orbit. This was expected as real-world wind conditions are turbulent in nature, and environmental effects are known to influence autopilot loiter tracking. Low-altitude flights operate in the atmospheric boundary where homogeneous turbulence is always present. This turbulence is significant, even at low wind speeds, as the relative size, weight, and scale of both the UAV and package allow for significant fluid energy transfer, perturbing the UAV and package movement. Accurately modelling the turbulence within the operating environment requires complex modelling methods outside the scope of this current research. However, including some form of flow disturbance to provide a better environmental representation is of interest and part of ongoing research. In both flight tests, the UAV trajectory drifts around a mean loiter radius with movements up to two standard deviations from the mean. The tracking of the UAV remains particularly circular even though deviation from the target loiter is experienced. The greatest error in loiter tracking is when the aircraft moves from the tailwind to the headwind condition, where it overshoots the target loiter

radius and consistently does this with each loiter rotation.

Figure 3 shows the package trajectory for an average wind condition of $2.07\,m/s$ at UAV level. The mean loiter radius of the UAV is $29.39\,m$ with a standard deviation of $1.94\,m$. As the flight-test UAV trajectory approaches one standard deviation from the mean, the corresponding flight-test package trajectory matches the predicted trajectory. For the majority of the flight time, the horizontal component of the flight-test package trajectory sits within this predicted region, with a slight shift in the westerly direction to what our model predicts.

There are greater tracking errors in altitude. Our assumption for the simulator is that the UAV can hold its altitude for the mission's duration. However, as can be seen, there is a variation of approximately five metres for this test. The flight test data shows a rotation of the horizontal plane about an axis perpendicular to the wind direction, with the peak altitude occurring as the UAV transitions from a tailwind to a headwind and dips at the opposite point. This can be explained due to the presence of wind. With wind, the package and UAV are loitering around different locations on the North East plane. As the UAV is flying away from the package, the tension in the tether increases as the relative distance between the package and the UAV increases. This additional force causes the UAV to be "pulled" down, causing the reduction in altitude. The autopilot then increases the throttle to regain altitude. Still, as the UAV continues the loop and transitions back toward the package, the tension in the tether minimises due to the distance between the package and the UAV decreasing. The result is that the UAV, with increased velocity, overshoots the altitude mark and reaches a peak altitude closest to the package before starting the same cycle again for the next rotation. This effect can be adjusted by altering the UAV's PID control parameters.

The effect of this flight path on the package trajectory produces an interesting effect. In simulation, the package trajectory shows this horizontal plane rotation about an axis perpendicular to the wind direction. This is damped out in the experimental data, with a more horizontal flight path. There is still an altitude variation of approximately eight metres, still within the bounds of the simulator's predicted region. Merz et al. [12] discussed this situation, where they concluded that to counter the vertical translation of the package in windy conditions, the UAV should alter its altitude to compensate. However, it appears that, even without programming this feature into the autopilot, there is a natural tendency to perform this manoeuvre due to the tether/UAV interaction.

Figure 4 shows the trajectory and package results for gentle breeze conditions. The UAV's mean loiter radius is $31.86\,m$ with a standard deviation of $3.84\,m$. With a doubling in wind velocity, the variation between predicted and observed flight paths of the UAV and package increases; however, the majority of the flight behaviour and dynamics are maintained from both the UAV and package. The UAV shows a greater variation in maintaining tracking in the turn from the tailwind to the headwind condition in a constant

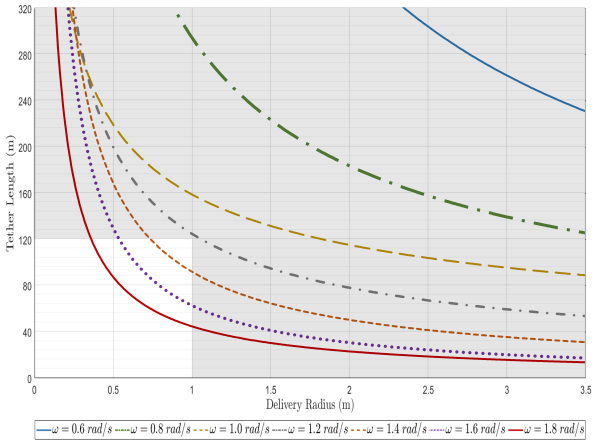

Fig. 5. Delivery radius vs. tether length as a function of radial velocities

attempt to maintain the target loiter profile. The package traverses beyond two standard deviations with a maximum radius of 27 metres, significantly more than the average predicted variance in simulation. This suggests that both the wind speed and turbulence experienced by the tether and package provide significant disturbance. Although the UAV moves between a larger standard deviation within the horizontal plane, the flight-test package trajectory corresponds to the predicted horizontal trajectory at each standard deviation. In the vertical plane, the observations are similar to the light breeze conditions. That is, the flight-test package remains within the predicted envelopes when accounting for the vertical movement of the UAV. We conclude our model suitably predicts the likely region of the package, and thus, our model is experimentally verified for low-wind conditions without the MTDD.

V. Simulation Results of the MTDD

We present the predictions of our model in simulation to demonstrate why the MTDD is required, shown in Figure 5. We model various loiter rates, ω, for various tether lengths and measure the radius of the package's orbit. The white area represents dynamics which fit within ICAO requirements (UAV operating under $120\,m$) and a suitably small package radius for collection (under $1\,m$). A valid delivery can be achieved for sufficiently high ω, corresponding to small loitering radii and high velocity turns. This causes high aircraft structural loading, which may exceed the UAV's structural limitations and cause a high power draw that reduces the UAV's mission time. We target values of $\omega < 0.8\,rad/s$ to avoid incurring unnecessary structural damage. Therefore, it's of great benefit to minimise the loiter rate and thus necessitates a MTDD.

Figure 6 shows the impact of the MTDD in ideal conditions without wind, where the MTDD is placed at 60% along the length of the tether. This highlights the significant change in the dynamics of the tether and orbit of the package. The additional drag of the MTDD moves the tether closer to the centre of the orbit at the location of the MTDD. After this point, the remaining tether is reduced to smaller orbit

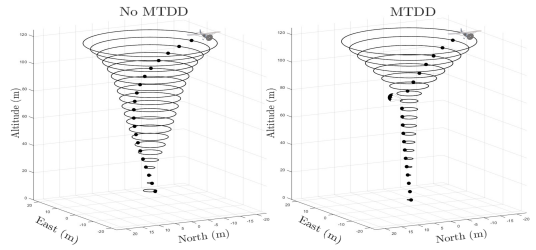

Fig. 6. Simulation results depicting the steady state tether system without a MTDD, left, vs. the same steady state simulation with a MTDD, right.

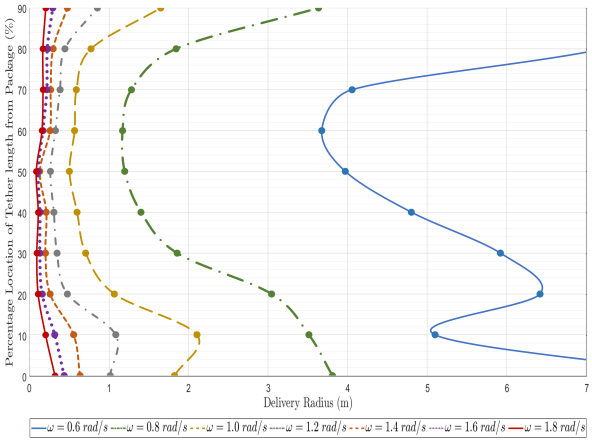

Fig. 7. Effect on the package delivery radius at different radial velocities with different MTDD locations up the tether, measured from the package

radii. The package orbital radius is significantly reduced, demonstrating the MTDD benefit.

We consider different positions of the MTDD on the tether. Figure 7 shows how the orbital radius of the package changes for different ω as the MTDD is moved along the tether, which is held at a constant $120\ m$. A position of 0% is the same as being without the MTDD attached. The MTDD has the greatest benefit when placed between the 50% and 70% of the tether length. This is intuitive given the tether dynamics without a MTDD shown in Figure 6. A MTDD at 10% of the tether length would not be effective as the tether already has a small orbit velocity and radius. Alternatively, attaching the MTDD at a high percentage would not allow the MTDD to move the tether to the orbital centre sufficiently to see any great effect. Rather, the MTDD would trail behind the UAV, causing larger power demands. Figure 7 also shows improvement across all radial velocities with more significant impacts at lower velocities. We concluded that setting the MTDD position to 60% for all situations will yield the best results, thus eliminating the need for adjustment during missions. These findings also reinforce minimising ω and the load on the UAV.

To demonstrate that the MTDD permits the UAV to work within ICAO and structural limitations, we model various loiter rates, ω, for various tether lengths and measure the radius of the package's orbit, with the MTDD positioned at 60% of the tether length. Figure 8 shows that the MTDD reduces the required loiter rates so that velocities of $\omega \geq$

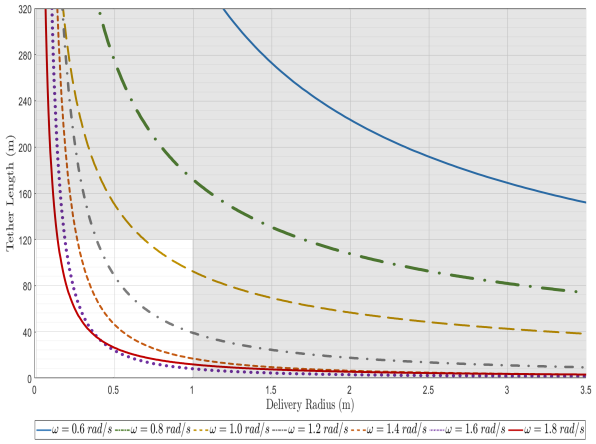

Fig. 8. Effect on the package delivery radius for different tether lengths at various radial velocities with a MTDD at 60% tether length

$1.0 rad/s$ now fall within the acceptable (unshaded) window, allowing deliveries to be achieved at lower radial velocities. The impact is reduced power consumption, resulting in more battery power being available to increase the UAV's range and endurance. It also means that heavier packages can be flown as the structural load from loitering can be traded for carrying capacity.

VI. Conclusions and Future Work

We present a novel design of a fixed-wing tethered package delivery UAV that employs a Mid-Tether Drag Device (MTDD). The MTDD has the possibility to enable the UAV, while flying a circular orbit above a delivery location, to stabilise the orbit of the package to within an acceptable parameter of $< 1\ m$ radius. We show that the MTDD can enable a fixed-wing aircraft to be a viable option as a delivery vehicle for long-range delivery missions, as the loiter radius during delivery can be reduced. This enables the UAV to be lighter, reduce structural demand during the delivery phase, conduct slower turns, carry more mass onboard, and require less energy from the motor, leaving more energy for missions. These results also align with ICAO regulations of a $120\ m$ flight ceiling. We present a model of our UAV dynamics, including the MTDD, and implement this model in a MATLAB® simulation. We experimentally verify and validate the outputs of our model and simulation with real-world field tests in environmental conditions similar to those acceptable for this type of mission. With our simulation model, we demonstrate the impact of our novel MTDD, and show the MTDD is optimally placed at 60% of the tether length. Our results enable us to build on the deployment mechanism of the MTDD in future work so that we can conduct flight tests with the MTDD at the optimal location to experimentally test the model and prove the concept in real-world flight conditions. This paper has discussed the key findings relating to the system; future work will expand on these findings with further investigation into other characteristics.

ACKNOWLEDGMENT

This research is funded by iMOVE CRC and supported by the Cooperative Research Centres program, an Australian Government initiative. The authors would also like to thank the RMIT UAS Research Team for supporting and guiding this project. We acknowledge the Greensborough Model Aircraft Club, where the field tests were conducted.

REFERENCES

[1] ICAO, "ICAO Model UAS Regulations," International Civil Aviation Organization," Report, 2020. [Online]. Available: https://www.icao.int/safety/UA/Pages/ICAO-Model-UAS-Regulations.aspxhttps://www.icao.int/safety/UA/Pages/default.aspx

[2] Statista, "Retail e-commerce sales worldwide from 2014 to 2024," https://www.statista.com/statistics/379046/worldwide-retail-e-commerce-sales/, 2021, accessed: 3/9/2021.

[3] A. A. Juan, C. A. Mendez, J. Faulin, J. De Armas, and S. E. Grasman, "Electric vehicles in logistics and transportation: A survey on emerging environmental, strategic, and operational challenges," *Energies*, vol. 9, no. 2, p. 86, 2016.

[4] Wing Aviation LLC., "Wing," 2024, Feb. 23, 2024. [Online]. Available: https://wing.com/

[5] P. Beigi, M. S. Rajabi, and S. Aghakhani, "An overview of drone energy consumption factors and models," *Handbook of Smart Energy Systems*, pp. 1–20, 2022.

[6] R. T. Hitt, *Jungle Pilot: The Story of Nate Saint, Martyred Missionary to Ecuador*. Our Daily Bread Publishing, 2017.

[7] ICAO, "Circular 328, unmanned aircraft systems (uas)," *Montreal, Canada: International Civil Aviation Organization (ICAO)*, 2011.

[8] S. L. Huang, "Mathematical model for long cable towed by orbiting aircraft," NAVAL AIR DEVELOPMENT CENTER WARMINSTER PA AERO MECHANICS DEPT," Report, 1969.

[9] R. A. Skop and Y.-I. Choo, "The configuration of a cable towed in a circular path," *Journal of Aircraft*, vol. 8, no. 11, pp. 856–862, 1971.

[10] M. Merz and T. A. Johansen, "Feasibility study of a circularly towed cable-body system for uav applications," in *2016 International Conference on Unmanned Aircraft Systems*. IEEE, 2016, pp. 1182–1191.

[11] M. Merz, "A strategy for robust precision control of an endbody being towed by an orbiting uav," in *AIAA Guidance, Navigation, and Control Conference*, 2017, p. 1040.

[12] M. Merz and T. A. Johansen, "Optimal path of a UAV engaged in wind-influenced circular towing," in *2017 Workshop on Research, Education and Development of Unmanned Aerial Systems*. IEEE, 2017, pp. 25–30.

[13] ——, "Control of an end body towed by a circling unmanned aerial vehicle," *Journal of Guidance, Control, and Dynamics*, vol. 42, no. 12, pp. 2677–2686, 2019.

[14] P. Williams and P. Trivailo, "Dynamics of circularly towed aerial cable systems, part 2: Transitional flight and deployment control," *Journal of Guidance, Control, and Dynamics*, vol. 30, no. 3, pp. 766–779, 2007.

[15] ——, "Dynamics of circularly towed aerial cable systems, part i: Optimal configurations and their stability," *Journal of Guidance, Control, and Dynamics*, vol. 30, no. 3, pp. 753–765, 2007.

[16] P. Lapthorne and P. Trivailo, "Flying: With strings attached," *Journal of Guidance, Control, and Dynamics*, vol. 32, no. 2, pp. 633–635, 2009.

[17] S. F. Hoerner, "Fluid-dynamic drag," *Hoerner fluid dynamics*, 1965.

[18] Y.-i. Choo and M. J. Casarella, "A survey of analytical methods for dynamic simulation of cable-body systems," *Journal of Hydronautics*, vol. 7, no. 4, pp. 137–144, 1973.

[19] National Oceanic & Atmospheric Administration, "LLLJP Wind Shear Formula," csl.noaa.gov. [Online]. Available: https://csl.noaa.gov/projects/lamar/windshearformula.html

[20] MATLAB, "Matlab version: 23.0.2 (r2023b)," Natick, Massachusetts, United States, 2023. [Online]. Available: https://www.mathworks.com

[21] ArduPilot, "Ardupilot version: 4.4.4," 2024. [Online]. Available: https://www.ardupilot.org

[22] D. Wheeler and C. Wilkinson, "From calm to storm: the origins of the beaufort wind scale," *The Mariner's Mirror*, vol. 90, no. 2, pp. 187–201, 2004.